Technology and Health Care 23 (2015) S285–S291
DOI 10.3233/THC-150964
IOS Press

Research on an anti-motion interference algorithm of blood oxygen saturation based on AC and DC analysis

Jiayun Yan and Guangyu Bin*
College of Life Science and Bio-engineering, Beijing University of Technology, Beijing, China

Abstract.
BACKGROUND: There is an urgent need for blood oxygen saturation (SpO2) tests when participants are ambulatory, as in daily activity monitoring, sleep monitoring, or even athletes' cardiovascular function tests. In such situations, measuring equipment needs to be wearable. This restricts the processor volume, and the corresponding algorithm should be microprocessor compatible.
OBJECTIVE: This article proposes an anti-motion interference blood oxygen saturation algorithm for the microcontroller based on AC and DC analysis, named de-trended FFT.
METHODS: An experiment was conducted to compare the de-trended FFT algorithm with two other algorithms commonly used in the time and frequency domains. In the experiment, participants' oxygen saturation levels were calculated from Photoplethysmography (PPG) signals that were recorded continuously. Meantime, five types of hand motions were conducted, including hand trembling movements, horizontal hand movements, vertical hand movements, finger tapping, and finger bending, with each state lasting 2 minutes.
RESULTS: Results show significant performance of de-trended FFT in SpO2 calculation ($P < 0.05$), in both accuracy and stability.
CONCLUSION: De-trended FFT stands out in both mean deviation and variance by eliminating trending influence when compared with the other two algorithms. The motion interference's influence on SpO2 calculation mainly comes from the AC component, not the DC.

Keywords: PPG, blood oxygen saturation, spO2, motion artifact

1. Introduction

In recent years, wearable medical devices have been used to continuously monitor vital human signals and further prevent deterioration by providing automatic notification services in emergency situations [1]. There is an urgent need for dynamic detection of blood oxygen using wearable devices [2,3]. If blood oxygen can be measured precisely by wearable equipment during sleeping, doctors or researchers can be notified in time when apnea occurs [4–7]. If blood oxygen can be monitored in daily activities, users can move freely while wearing the equipment; this will assist doctors in diagnosing potential phenomenon and treating patients as soon as possible [8]. If blood oxygen can be measured during exercise, the athlete's cardiovascular function can be evaluated by SpO2 changes. However, the detection results

*Corresponding author: Guangyu Bin, No. 100 Pingleyuan, Chaoyang District, Beijing, China. Tel.: +86 13811135094; E-mail: guangyubin@qq.com.

of wearable devices are always affected by body movement; this problem has not been solved well enough by existing products.

Generally, SpO2 detection requires participants to remain still so that the peak and valley of Photoplethysmography (PPG) [9,10] can be measured based on the good quality of the waveform. In movement states, participants' gesture changing and breathing all lead to baseline drift of the PPG signal, which makes it difficult to detect the peak and valley of the PPG, ultimately affecting the accuracy and stability of the blood oxygen test [11]. Restricting participants' activity also limits the SpO2 detection's application scenarios.

Recent research has made great breakthroughs in eliminating motion artifact and reconstructing PPG signals, such as smoothed pseudo winger-ville distribution (SPWVD), singular value decomposition (SVD) and cycle-by-cycle Fourier series analysis (CFSA). SPWVD removes the effects of motion artifact through the three-dimensional distribution of time, frequency and energy [12]. SVD and CFSA both extract characteristic from a single cycle, eliminating movement interference, and further reconstructing signal without interference. In this way, all morphological characteristics of the original PPG signal can be reserved [13,14], and stable blood oxygen is calculated, making SVD and CFSA stand out from other methods. However due to their high computing complexity, neither SPWVD, SVD, nor CFSA are suitable for the microcontroller.

In this paper, an anti-motion interference SpO2 algorithm is proposed and named de-trended Fast Fourier Transform (de-trended FFT). This algorithm aims to eliminate the effects of motion artifact by de-trended analysis and post processing analysis, based on FFT. We believe that motion interference's influence on SpO2 calculation mainly comes from the AC component in FFT.

2. De-trended FFT SpO2 algorithm

Two kinds of light sources, red and infrared light, are collected by equipment in SpO2 detection, forming two PPG signals. The PPG's peak and valley values are commonly utilized in computing blood oxygen saturation [15,16]. In accordance with the theory that oxyhemoglobin (HbO2) and deoxygenated hemoglobin (DHb) have different extinction coefficients for both red and infrared light [2], oxygen saturation can be calculated with an empirical formula of the normalized ratio R. R is an odds ratio, in which the numerator is the ratio between the red light's AC and DC components while the denominator is the ratio between the infrared light's AC and DC components, representing the ratio between the red light's transmitted light intensity and infrared's. Ratio R is given below as

$$\mathrm{R} = \frac{(\mathrm{I_{AC}/I_{DC}})_{\mathrm{RED}}}{(\mathrm{I_{AC}/I_{DC}})_{\mathrm{IR}}} = \frac{(\mathrm{I_{RED}/I_{IR}})_{\mathrm{AC}}}{(\mathrm{I_{RED}/I_{IR}})_{\mathrm{DC}}} \tag{1}$$

Obviously, the precision and stability of the AC and DC components' calculation is the most vital issue. Before the de-trended FFT algorithm was put forward, a series of test was carried out to find a better way to obtain AC and DC, including finding peak and valley values of PPG, filters, and FFT. In accordance with test results, it is difficult to find peak and valley from PPG, so this method is not the best choice. Interestingly, the FFT's DC calculation results almost totally coincide with the low pass filter, illustrating that motion interference does not exert any influence on the DC components in SpO2 computing. Thus it is estimated that calculating the AC parts is the key point in calculating SpO2. To confirm this estimation, FFT on raw PPG (group 1) and on the de-trended signal (group 2) was carried out; Fig. 1 shows the calculation results. Results show that group 2 vibrated more mildly than group 1, especially in parts where the original signal changes violently.

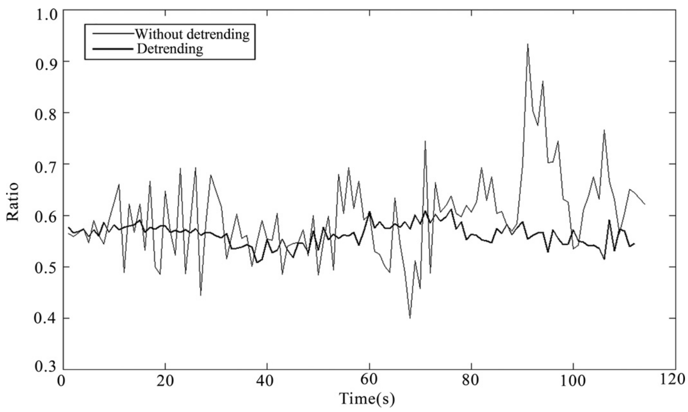

Fig. 1. AC-components ratio of red and infrared light.

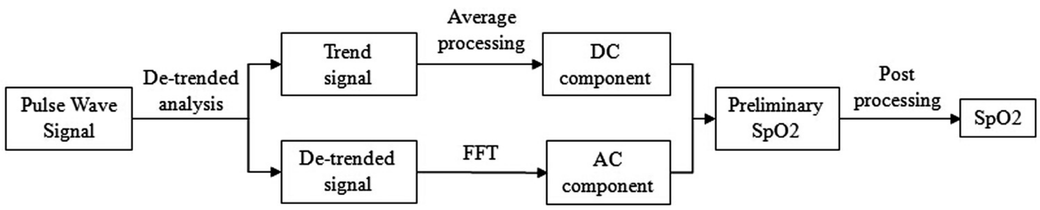

Fig. 2. Block diagram of the optimized de-trended FFT algorithm.

As shown in Fig. 2, raising the de-trended algorithm consisted of three parts: 1) de-trended analysis, 2) FFT, 3) post processing analysis.

Initially, de-trended analysis mainly removes the PPG baseline, that is the parts at a frequency of approximately 0 Hz in the frequency domain. To yield the DC component, a second-order Butterworth low-pass filter was chosen with a cut-off frequency at 0.5 Hz. The rest of the components in the original PPG are called the de-trended signal, which could further come into the AC component through FFT. For the part of FFT, the strongest spectral line within the cardiac frequency band (1–2 Hz) is selected for the AC components, corresponding to pulse components ranging from 60 beat/min to 120 beat/min. FFT is executed in every 8 second PPG period that overlaps 1 second with another period [17,18] at a sample rate of 128 Hz. Finally, post processing analysis, which includes standard averaging and singularity elimination, further improves the accuracy of SpO2 calculation. Standard averaging here is the four-point weighted moving average, which aims to further stabilize the calculated SpO2. If SpO2 variation is higher than 2% within a second, the SpO2 value is considered singular and is discarded, because physiology makes it impossible for SpO2 to change abruptly.

3. Experiment and results

3.1. Experimental protocol

The experiment is under the Declaration of Helsinki (2000) of the World Medical Association and the protocols are approved by the Institutional Research Review Board at the Hospital of the Beijing University of Technology. In addition, the experimental participants gave informed consent.

For the experiment, ten healthy participants were selected, five males and five females, aged 22 to 26. Participants were required to perform five kinds of motion while wearing a PPG sensor on the middle finger of their right hand. They performed each motion for two minutes, during SpO2 detection. Here, red and infrared light was collected at sample rate of 128 Hz. In addition, the PPG of the left hand was detected using the same sensor as the control group. Complicated hand motions were classified into the five basic action types to quantize the control of exercise intensity conveniently and explore the effects of different motions on SpO2. Among the five motions, horizontal movement and vertical movement simulate the fundamental movement of an arm, with high amplitude and low frequency. Finger bending is performed as the most basic motion of the finger. Trembling movements mainly simulate the behavior of patients with Parkinson's disease. Finger tapping represents situations where the finger hits something in daily life. For comparison, results from a stationary state were also recorded. Motions were conducted at a frequency ranging from 0.5 Hz to 4 Hz during SpO2 measurement. The amplitude scope of horizontal hand movements and vertical hand movements was from 5 cm to 7 cm, and the scope of other types from 2 cm to 5 cm.

3.2. Data processing

The purpose of this experiment is to compare the performances of the commonly used time-domain SpO2 algorithm, the frequency-domain algorithm, and de-trended FFT. SpO2 is calculated using the time-domain algorithm via the peak and valley, which is determined by the maximum and minimum of the single PPG wave. In this article, the frequency-domain method is FFT, and it is introduced in the de-trended FFT algorithm above. Similarly, time-domain and frequency-domain also yield a SpO2 value every 8 seconds, which overlaps each 1-second piece with another.

SpO2 values do not change rapidly for healthy people in a relatively short time if participants are not doing strenuous exercise, confirmed by the medical oximeter on the left hand. Therefore, the SpO2 value from participants' right hand is considered stable despite the fact that the right hand is in motion. In order to evaluate the effects of the three different algorithms, the precision and variance of the calculated SpO2 are analysed. Precision is depicted by the mean deviation between participants' measured values and standard values (offered by the oximeter tied to the left hand). SpO2 variance indicates the algorithms' stability. A T-test is conducted to discern which approach presents the best consequence in SpO2 calculation.

3.3. Results

As shown in Table 1, among the three algorithms, the time-domain method has the highest mean deviation and de-trended FFT and FFT are very close to each other, while the former is smaller in general. On the other hand, variance of the de-trended FFT is relatively low compared with the time-domain algorithm and FFT in all states of motions. A T-test was conducted between each pair of the three algorithms in the same motion condition, and P values are less than 0.05 in all but three cases. In one of these cases, the P value between the FFT algorithm and the de-trended FFT was 0.1583 in trembling movement and the P value between the time-domain algorithm and the de-trended FFT in bending movement was 0.079, which may be caused by the high variance of time-domain results, because the P value between the time-domain algorithm and FFT was also more than 0.05. The results illustrate that, in most cases, the de-trended FFT shows significant improvement from the time-domain method and FFT in both accuracy and stability of SpO2 computation.

Table 1
Mean deviation of three kinds of algorithm

	Still	Trembling	Vertical	Horizontal	Tapping	Bending
Time-domain	−0.106	−6.219	−3.528	−2.838	−1.343	−8.4
FFT	−0.121	−0.105	−0.446	−0.531	−0.748	−1.885
De-trended FFT	−0.081	0.034	−0.321	−0.44	−0.685	−1.708

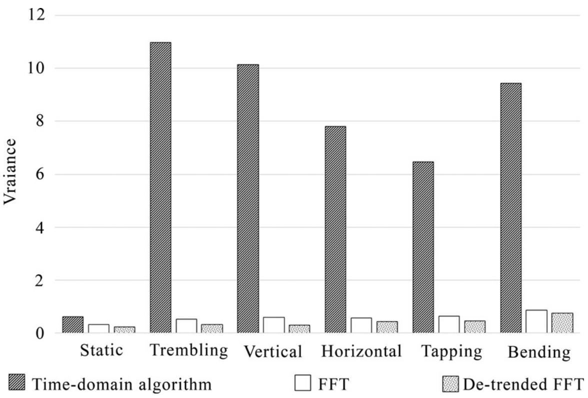

Fig. 3. The variance of SpO2 using time domain algorithm, FFT and de-trended FFT algorithm in the six states of motion.

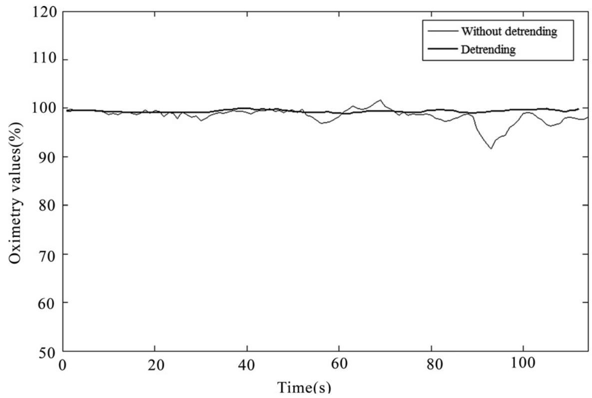

Fig. 4. SpO2 calculated by de-trended and commonly used method.

4. Discussion

The mean deviation represented how severely the habitual movements simulated by the five different motions used in this study interfere with the measured results. As shown in Table 1, hand motions cause the time-domain results to deviate very severely from the true value, and may even be meaningless for clinical diagnosis. This implies that the effects of exercise on SpO2 detection are significant enough. Among the five habitual movements, the bending movement caused the most deviation, no matter which method was used. Trembling scarcely influenced the blood oxygen's deviation with the frequency-domain or de-trended FFT algorithms, but exerted high effects on the time-domain method. Surprisingly, tapping did not affect SpO2 precision as expected.

Notably, several participants' SpO2 deviated severely beyond the normal range when using the time-domain algorithm in certain motion states. For example, the SpO2 value of participant No. 5 was 57% in the trembling movement. The corresponding original pulse waveform was seriously affected by motion; thus the accurate peaks and valleys of pulse waves could not be found, whereas relatively precise SpO2 values could be calculated by FFT and de-trended FFT. Results demonstrated that AC and DC components could not be detected in the time domain under the effect of motion but could be found in the fixed spectral band in the frequency domain.

De-trended FFT was better in both precision and stability than FFT, as shown in Table 1 and Fig. 3. De-trended FFT's better performance may be due to the de-trending procedure. For further research, the curves of SpO2 calculated by de-trended FFT and FFT were plotted in Fig. 4, and the example data is in accordance with that of Fig. 1. The improved parts by de-trended FFT in the SpO2 curve match that of the curves of the AC-components ratio (Fig. 1), especially for the greater fluctuation between the 80 s and 100 s in Figs 1 and 4. Therefore, it seems that improving AC calculation contributes directly to better SpO2 results.

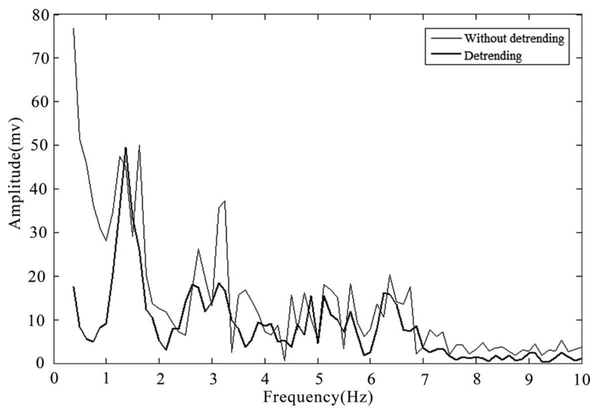

Fig. 5. FFT spectrum of red.

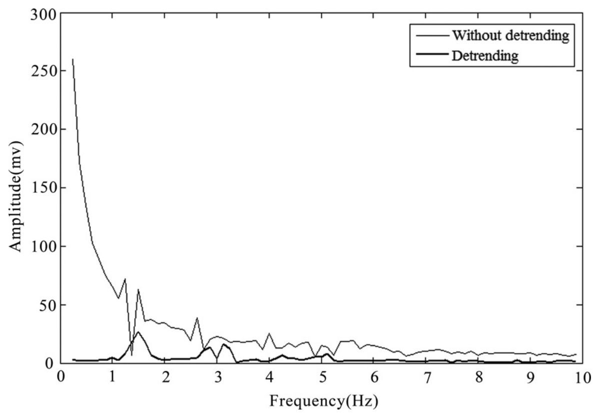

Fig. 6. FFT spectrum of IR.

This study also demonstrates that the influence of the motion is mostly applied to the AC components of PPG. For FFT, the raw PPG signal ought to be weakly stationary before processed; however, in practical applications, the SpO2 signal showed slow linear changes or more violent, complicated trend. Spectrum analysis conducted in such conditions may lead to distortion of time-frequency analysis. Figures 5 and 6 show signal fragments with intense baseline drift that were picked on which FFT was carried before de-trending and after.

As the amplitude of the DC components is far greater than that of the AC components, those DC components would cause certain effects on spectra converter results, especially for the frequency band ranging from 1 Hz to 2 Hz. Under such conditions, poor AC component extraction leads to unstable oxygen calculations. After the de-trending process, the peak from frequency band 1 Hz to 2 Hz is easier to find.

The differences between the reviewed algorithm and de-trended FFT are also discussed here. De-trended FFT calculates SpO2 from two dimensions, time and frequency, whereas SPWVD is based on three-dimensional distribution and further calculates SpO2 through the dispose-adding window. Obviously, the latter method of computing is more complex. Similarly, both SVD and CFSA have more computational complexity than the algorithm put forward in this article. Thus, the de-trended FFT algorithm would simplify programming and improve microprocessors' operational efficiency. At the same time, the de-trended FFT algorithm improves calculation accuracy and especially stability, as shown in Figs 3 and 4. In Fig. 4, the curves of the de-trending method hardly fluctuate, while those from FFT without de-trending do. High stability contributes to the precision of SpO2 continuous monitoring. As we can see, the precision and stability of de-trended FFT algorithm are high enough to meet the demand of detection in motion. Based on its high precision and simplicity, the de-trended FFT algorithm can be applied in embedded systems as a lightweight SpO2 algorithm in motion.

The restriction of the de-trended FFT algorithm is that it cannot acquire more parameters from the reconstructed pulse wave, like SVD and CFSA can. However, if only SpO2 is needed, using SVD and CFSA is a waste of computing resources.

5. Conclusion

In an attempt to improve the current algorithm for SpO2 calculation, this study puts forward the de-trended FFT algorithm to avoid the influence of severe baseline drift on PPG in states of motion. The de-trended FFT algorithm stood out in the experiment, especially in the cases of stationary states, trembling and finger tapping. The performance of SpO2 calculation improves significantly in both accuracy and stability. In addition, what needs to be emphasized is that movement interference only impacts the AC component of PPG, not the DC component, which leads inaccurate SpO2 computing. De-trended analysis based on FFT gives a great result of the extraction on the AC component, which is the main factor in obtaining better SpO2 computing results. Further work is required to research the AC component in motion, by which baseline drift may be fundamentally solved. Comparison between de-trended FFT, SPWVD, SVD and CFSA in the field of calculation precision is also a promising future project.

References

[1] Reddy KA, George B, Kumar VJ. Use of fourier series analysis for motion artifact reduction and data compression of photoplethysmographic signals. Instrumentation and Measurement, IEEE Transactions on, 2009, 58(5): 1706-1711.
[2] Hayes MJ, Smith PR. A new method for pulse oximetry possessing inherent insensitivity to artifact. Biomedical Engineering, IEEE Transactions on, 2001, 48(4): 452-461.
[3] Hayes MJ, Smith PR. Artifact reduction in photoplethysmography. Applied Optics, 1998, 37(31): 7437-7446.
[4] Wang CW, Hunter A, Gravill N, et al. Unconstrained video monitoring of breathing behavior and application to diagnosis of sleep apnea. Biomedical Engineering, IEEE Transactions on, 2014, 61(2): 396-404.
[5] Hwang SH, Lee HJ, Yoon HN, et al. Unconstrained Sleep Apnea Monitoring Using Polyvinylidene Fluoride Film-Based Sensor. 2014.
[6] Georgiou HV. Adaptive detection and severity level characterization algorithm for Obstructive Sleep Apnea Hypopnea Syndrome (OSAHS) via oximetry signal analysis. arXiv preprint arXiv:1308.6203, 2013.
[7] Zhang J, Zhang Q, Wang Y, et al. A real-time auto-adjustable smart pillow system for sleep apnea detection and treatment. Information Processing in Sensor Networks (IPSN), 2013 ACM/IEEE International Conference on. IEEE, 2013: 179-190.
[8] Foo JYA. Use of independent component analysis to reduce motion artifact in pulse transit time measurement. Signal Processing Letters, IEEE, 2008, 15: 124-126.
[9] Rusch TL, Sankar R, Scharf JE. Signal processing methods for pulse oximetry. Computers in Biology and Medicine, 1996, 26(2): 143-159.
[10] Ram MR, Madhav KV, Krishna EH, et al. A novel approach for motion artifact reduction in PPG signals based on AS-LMS adaptive filter. Instrumentation and Measurement, IEEE Transactions on, 2012, 61(5): 1445-1457.
[11] Maeda Y, Sekine M, Tamura T. Relationship between measurement site and motion artifacts in wearable reflected photoplethysmography. Journal of Medical Systems, 2011, 35(5): 969-976.
[12] Yan Y, Poon CCY, Zhang Y. Journal of NeuroEngineering and Rehabilitation. Journal of NeuroEngineering and Rehabilitation, 2005, 2: 3.
[13] Kanjilal PP, Palit S. On multiple pattern extraction using singular value decomposition. IEEE transactions on signal processing, 1995, 43(6): 1536-1540.
[14] Reddy KA, Kumar VJ. Motion artifact reduction in photoplethysmographic signals using singular value decomposition. Instrumentation and Measurement Technology Conference Proceedings, 2007. IMTC 2007. IEEE. IEEE, 2007: 1-4.
[15] Yao J, Warren S. A short study to assess the potential of independent component analysis for motion artifact separation in wearable pulse oximeter signals. Engineering in Medicine and Biology Society, 2005. IEEE-EMBS 2005. 27th Annual International Conference of the. IEEE, 2005: 3585-3588.
[16] Couceiro R, Carvalho P, Paiva RP, et al. Detection of motion artifacts in photoplethysmographic signals based on time and period domain analysis. Engineering in Medicine and Biology Society (EMBC), 2012 Annual International Conference of the IEEE. IEEE, 2012: 2603-2606.
[17] Rusch TL, Scharf JE, Sankar R. Alternate pulse oximetry algorithms for SpO 2 computation. Engineering in Medicine and Biology Society, 1994. Engineering Advances: New Opportunities for Biomedical Engineers. Proceedings of the 16th Annual International Conference of the IEEE. IEEE, 1994: 848-849.
[18] Pflugradt M, Rose M, Orglmeister R. A Novel Method for Motion Artifact Removal in Wearable PPG Sensors Based on Blind Source Separation. Biomedical Engineering/Biomedizinische Technik, 2013.